WILEY-VCH

COMMUNICATION

Ion Mobility Mass Spectrometry for the Rapid Determination of the Topology of Interlocked and Knotted Molecules

Anneli Kruve,[a] Kenji Caprice,[b] Roy Lavendomme,[c] Jan M. Wollschläger,[a] Stefan Schoder,[a] Hendrik V. Schröder,[a] Jonathan R. Nitschke,*[c] Fabien B. L. Cougnon,*[b] and Christoph A. Schalley*[a,d]

Abstract: A rapid screening method based on traveling-wave ion mobility spectrometry (TWIMS) combined with tandem mass spectrometry provides insight into the topology of interlocked and knotted molecules, even when they exist in complex mixtures such as interconverting dynamic combinatorial libraries. A TWIMS characterization of structure-indicative fragments generated by collision-induced dissociation (CID) together with a floppiness parameter defined merely based on parent and fragment ion arrival times provide a straightforward topology identification. To demonstrate its broad applicability, this approach is applied here six Hopf and two Solomon links, a trefoil knot, and a [3]catenate.

Interlocked and knotted structures are familiar in our everyday life; examples range from shoe laces and chains to symbols in art carved into stone in ancient times.[1] Molecular knots are topologically complex, self-entwined rings, while catenanes, in topology also called links, are structures formed by at least two mechanically interlocked rings. The Briggs notation x_z^y differentiates unambiguously between different topologies, where *x* denotes the minimum number of nodes in the molecular graph, *y* the number of rings, and *z* the order of the structure.[2] For instance, the simplest [2]catenane, a Hopf link, is represented as 2_1^2 (Figure 1). Molecular knots and catenanes were discovered already decades ago; for example, bacteriophages pack DNA with almost the density of crystals by making use of knotted structures.[3] Dabrowski-Tumanski and Sulkowska recently showed knotted structures to be present also in several proteins that are stable at high temperatures.[4] Knots and catenanes have also become an important research field in supramolecular chemistry, not only motivated by the beauty of their structures, but also by their use as molecular machines.[5,6]

Often, it is a challenge to unambiguously establish interlocked and knotted topologies by standard spectroscopic techniques. NMR shifts are not always indicative of such a topology and peaks can be too broad to allow any clarity about the structure.[7,8] Also, CD spectroscopy has its limitations even though many knots are topologically chiral, as enantiomer separation is required after a racemic synthesis before CD spectroscopy can be applied.[9] Crystallography often provides the ultimate evidence for interlocked or knotted topologies. However, high-quality single crystals are needed, but frequently not easy to obtain.[10,11]

These analytical limitations become even more severe, when the knotted or catenated structures are formed in complex mixtures of (quickly) interconverting dynamic combinatorial libraries,[12] in which multiple species co-exist.[13] A change of conditions, *e.g.* temperature, pH, concentration, or solvent, may then lead to shifts of the equilibrium to other topologies.[2] For example, Prakasam *et al.*[14] observed a transformation of a trefoil knot into a Hopf link, when temperature was raised. Pentecost *et al.*[15] showed how sensitive such libraries can be to small changes. Borromean rings formed when the ligands used were equilibrated with either Zn(II) or Cu(II) templating metal ions. In marked contrast, a Solomon link forms when Zn(II) and Cu(II) are both added simultaneously. Such interconversions may prevent the separation of the desired compounds in order to obtain single crystals or good spectroscopic data. Consequently, there clearly is a need for a rapid screening method to probe the presence and unravel the topology of knots and catenanes even when they are present in complex mixtures.

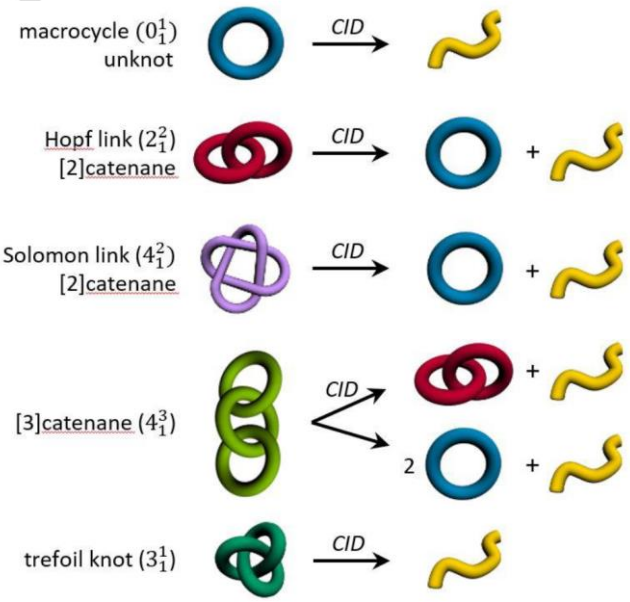

Figure 1. Topologies and Briggs notations of the different species under study. Structure-indicative fragmentation reactions expected to occur in CID/TWIMS experiments are shown schematically on the right.

Two different mass spectrometric approaches have been used to study molecular topology: In fortunate cases, structure-indicative fragmentation reactions in the gas phase

[a] Dr. A. Kruve, J. M. Wollschläger, Dr. S. Schoder, Dr. H. V. Schröder, Prof. C. A. Schalley
Institut für Chemie und Biochemie, Freie Universität Berlin
Takustrasse 3, 14195 Berlin (Germany)
E-mail: c.schalley@fu-berlin.de
[b] K. Caprice, Dr. F. B. L. Cougnon
Department of Organic Chemistry, University of Geneva
30 Quai Ernest Ansermet 1211 Geneva 4 (Switzerland)
E-mail: fabien.cougnon@unige.ch
[c] Dr. R. Lavendomme, Prof. J. R. Nitschke
Department of Chemistry, University of Cambridge
Lensfield Road, Cambridge CB2 1EW (UK)
E-mail: jrn34@cam.ac.uk
[d] Prof. C. A. Schalley
School of Life Sciences, Northwestern Polytechnical University
127 Youyi Xilu, Xi'an, Shaanxi 710072, P. R. China

Supporting information for this article is given via a link at the end of the document.

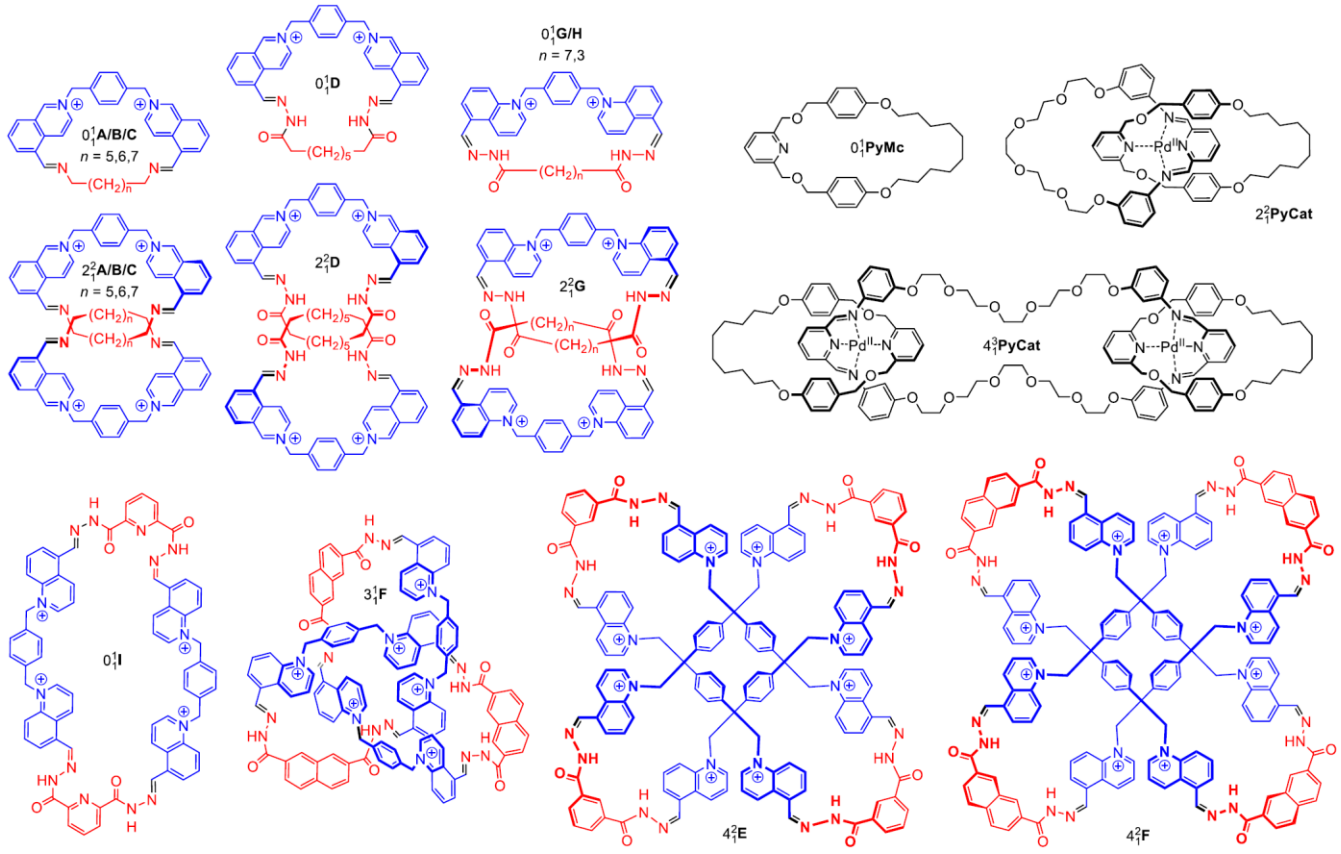

Figure 2. The structures of macrocycles 0_1^1**A**, 0_1^1**B**, 0_1^1**C**, 0_1^1**D**, 0_1^1**G**, 0_1^1**H**, and 0_1^1**I**, Hopf links 2_1^2**A**, 2_1^2**B**, 2_1^2**C**, 2_1^2**D**, and 2_1^2**G**, trefoil knot 3_1^1**F**, and Solomon links 4_1^2**E** and 4_1^2**F**, which form in different dynamic libraries **A** – **I** through Schiff base formation from the corresponding doubly charged dialdehyde (blue; counterion: Br^-) and the respective diamine or dihydrazide (red). For details, see Supporting Information. Macrocycle, [2]- and [3]catenates 0_1^1**PyMc**, 2_1^2**PyCat**, 4_1^3**PyCat** that assemble by subcomponent self-assembly are included to test, whether their topology can still be determined, when the catenate wheels are connected through metal coordination in addition to the mechanical bond.

provide evidence for catenane (or similarly rotaxane) formation.[16–18] This approach is, however, not easily applicable to knots, as they consist of a single macrocycle that opens upon bond cleavage into the same linear fragment as the corresponding unknot, thus also yielding the same fragmentation patterns. Alternatively, ion mobility mass spectrometry (IM-MS) has been used for the identification of catenanes by determining the collision cross section (CCS) of the intact parent ion of interest.[19,20] The experimental CCS can be compared with either the experimental CCS of independently prepared control compounds or with theoretical CCS values calculated for the topological isomers. Typically, interlocked or knotted structures are more compact than their non-intertwined analogues. Also, this approach has some limitations, as control compounds may not be readily available and thorough theoretical studies of large catenanes and knots are computationally intensive.

Recently, we have combined both approaches to characterize several Hopf links forming through imine bond formation in water within dynamic combinatorial libraries: Collision-induced dissociation (CID) was followed in these experiments by travelling-wave ion mobility mass spectrometry (TWIMS/MS) of the parent *and* fragment ions.[21] We now elaborate this approach into a rapid and general method for the determination of molecular topology by extending it to more complex intertwined architectures such as Solomon links, [3]catenates, and a trefoil knot (Figure 2). As our protocol is based on size and shape *differences* rather than absolute collision cross section data, there is no need for accurate cross section calibration, the determination of CCS data of control compounds or extensive calculations to obtain theoretical CCS values.

Figure 1 shows the fragmentation reactions expected to occur for different molecular topologies, when sufficient collision energy is provided in CID experiments to cleave a bond within one of the wheels. The cleavage of the first covalent bond opens one of the macrocycles. For the Hopf and Solomon links, one component can then disentangle from the other, leading to two fragments, one cyclic and one linear. If the two rings are identical, both fragments will have the same elemental composition and thus *m/z*, but will be different in their size. While the fragment masses alone do not lead to a conclusive assignment of intertwined structures, ion mobility spectrometry (IMS) can provide evidence that the two fragments differ in size. The catenated topology is confirmed by showing that one cyclic and one linear component form in the CID experiment. However, this raises the question of how to distinguish the Hopf from the Solomon link as both basically will behave analogously in the CID/IMS experiment.

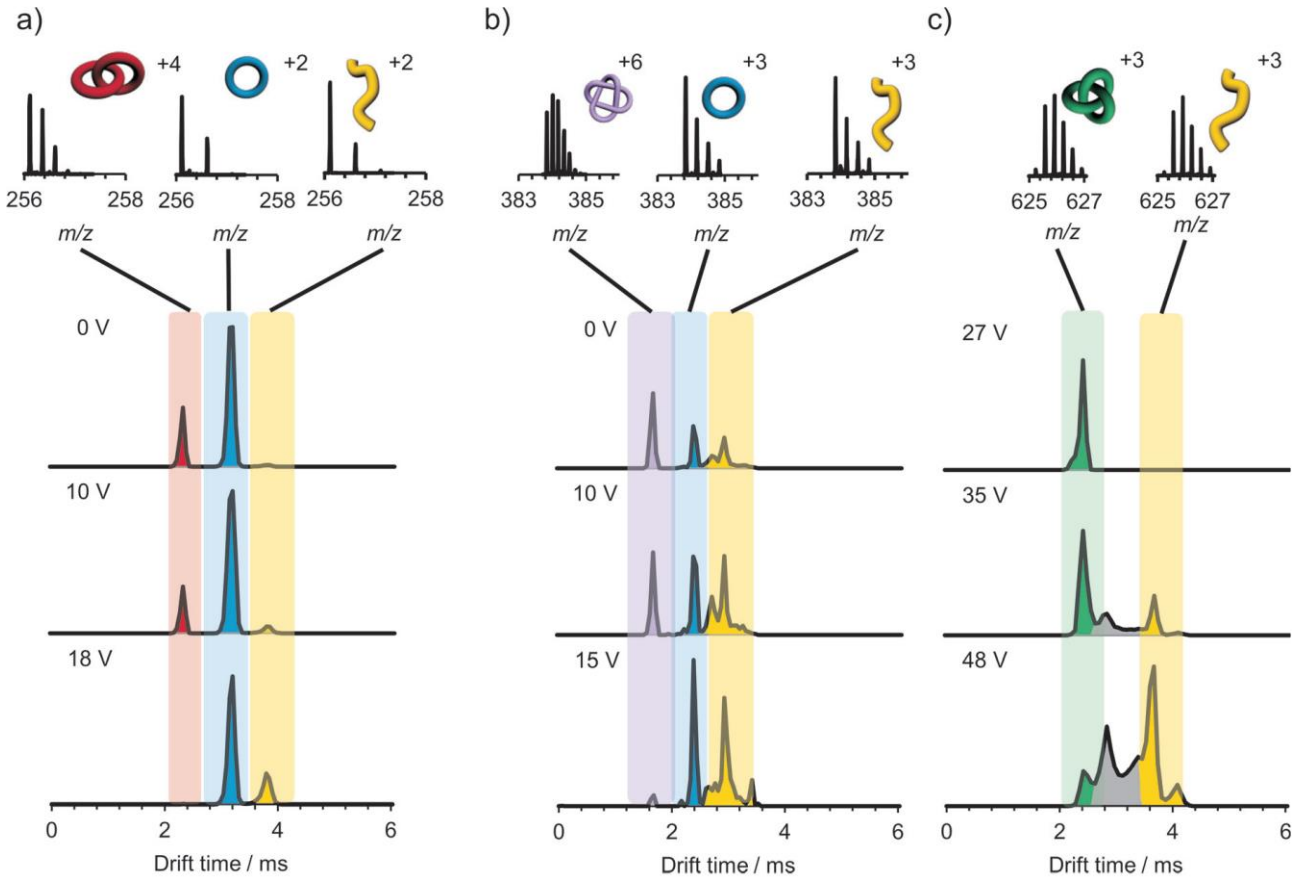

Figure 3. Normalized arrival time distribution of the species formed from (a) Hopf link $[2_1^2\mathbf{A}]^{4+}$, (b) Solomon link $[4_1^2\mathbf{E}-2H^+]^{6+}$, and (c) trefoil knot $[3_1^1\mathbf{F}-2H^+ + e^-]^{3+}$at low, medium and high collision voltage in the mass selected CID/IMS experiments. Library A contained both a Hopf link $[2_1^2\mathbf{A}]^{4+}$ and a macrocycle $[0_1^1\mathbf{A}]^{2+}$. The isotope patterns above demonstrate that the species formed from Hopf link and Solomon link carry half of the mass and half of the charge of the parent ion.

Solomon links are more extensively entangled and should thus be more densely packed and conformationally less flexible in their cores. Upon dissociation into the non-entangled fragments, less compact structures form. Consequently, we define a "floppiness factor" *Fl*, which simply divides the charge-corrected arrival time of the entangled parent by the mass- and charge-corrected arrival time of the least entangled fragment (typically the linear one):

$$Fl = \frac{t_{par}\cdot z_{par}}{t_{frag}\cdot z_{frag}} \cdot \left(\frac{M_{frag}}{M_{par}}\right)^{2/3} \quad (1)$$

In equation (1), *t* represents the arrival time in ms, *z* is the ion charge, and *M* its mass (*par* = parent, *frag* = fragment ion). The term $t_{frag}\cdot z_{frag}\cdot(M_{par}/M_{frag})^{2/3}$ can be regarded as the arrival time extrapolated from the (randomly folded) linear fragment to a randomly folded linear parent ion assuming isotropic growth (for details, see Supporting Information). Thus, the floppiness factor compares the experimental arrival time of the intertwined parent ion to the arrival time extrapolated for a randomly folded single-chain parent ion. Solomon links should, therefore, have a smaller floppiness factor as compared to Hopf links due to the higher degree of entanglement.

Similar considerations apply to the comparison of a non-intertwined macrocycle and trefoil knot. A knot opens into a linear fragment having the same *m/z* as the parent knot. Again, this is only detectable when IMS is capable of distinguishing the intertwined from the linear structure. The floppiness factor calculation can be applied again with $(M_{frag}/M_{par})^{2/3}$ = 1 as both ions have the same mass. As an advantage, *Fl* does not rely on absolute cross sections and can be quickly applied by simply using the measured arrival times.

Libraries A, B, C, D, and G were prepared by Schiff base condensation of the corresponding dialdehyde (blue subunits in Figure 2) with different diamines or dihydrazides (red subunits) in water at pH 9.6 (for details, see Supporting Information) and have been reported previously.[21–23] All of these libraries contain both, a macrocycle ($0_1^1\mathbf{A}$, $0_1^1\mathbf{B}$, $0_1^1\mathbf{C}$, $0_1^1\mathbf{D}$, and $0_1^1\mathbf{G}$) and the corresponding Hopf link ($2_1^2\mathbf{A}$, $2_1^2\mathbf{B}$, $2_1^2\mathbf{C}$, $2_1^2\mathbf{D}$, and $2_1^2\mathbf{G}$) in a dynamic equilibrium. Both, the doubly charged macrocycle and the quadruply charged Hopf link appear at the same *m/z* in the ESI mass spectra as indicated by their superimposed isotope patterns. All Hopf links fragment into one linear and one cyclic fragment that could be separated with TWIMS (shown for $2_1^2\mathbf{A}$ in Figure 3a as a representative example). The CID fragmentation reactions of the macrocycles and catenanes in libraries **A** – **C**

have been analysed in detail earlier and may serve here as representative examples.[21] Briefly, the C-N bond connecting the benzyl and (iso)quinolinium units easily opens as the ammonium ion is a good leaving group that creates a well stabilized benzylium ion when cleaved. Certainly, this is also the preferred cleavage site for the other compounds from libraries **D** – **I**. Analogously, the exclusive cleavage of the terminal macrocycles in $4_1^3\mathbf{PyCat}$ suggests that the benzylic C-O bond is the weakest one here. However, even without knowing exactly, which bonds are cleaved, the method described here can be applied. With increasing collision voltage, the peak of the Hopf link (but not that of the macrocycle) vanished in the mobilogram (Figure 3a) and a third peak for the linear fragment appears as evidenced by the m/z values and the isotope patterns that are identical for both fragments. The unchanged abundance of the macrocycle indicates that the fraction of it that is fragmented is replenished by the cyclic fragment formed upon fragmentation of the Hopf link.

To apply this protocol to more complex topologies, libraries E and F were investigated. Library E contains almost exclusively Solomon link $4_1^2\mathbf{E}$, whereas library F contained trefoil knot $3_1^1\mathbf{F}$ and a previously unidentified species,[23] which could be assigned as a Solomon link $4_1^2\mathbf{F}$ with the aid of CID/IMS considering the characteristic floppiness factor (vide infra for differentiation between Hopf and Solomon links). The Solomon links both consist of two identical rings and were observed in different charge states (z = +4 – +6) in the ESI mass spectra (Figure S14 and S17). Higher charge states are not observed because of (a) deprotonation of some of the hydrazone groups and (b) single-electron reductions at the ESI needle during ionization. Both processes help reduce charge repulsion within the naked ions in the gas phase.[24] The CID/IMS experiments reveal the expected isobaric linear and cyclic fragment ions (Figure 3b). For $[4_1^2\mathbf{E}^{8+} - 2H^+]^{6+}$, increasing collision voltages result in the formation of a linear $[0_1^0\mathbf{E}^{4+} - 1H^+]^{3+}$ and a cyclic $[0_1^1\mathbf{E}^{4+} - 1H^+]^{3+}$ fragment. Clearly, CID experiments can be used to provide conclusive fragmentation patterns.

The trefoil knot present in library F is observed in the ESI mass spectra as the $[3_1^1\mathbf{F} - 2H^+]^{4+}$ ion. The CID experiment conducted with this ion resulted in a fragmentation into species with lower *m/z* and lower drift times. This phenomenon is likely to result from the high entanglement and simultaneous high charge repulsion in the $[3_1^1\mathbf{F} - 2H^+]^{4+}$ ion, which does not allow the knot to untangle sufficiently before cleavage of the next covalent bonds occurs and the unfolded linear fragment can be formed. To overcome this issue, the knot was first subjected to electron-transfer dissociation (ETD) which gave rise to an ion $[3_1^1\mathbf{F} - 2H^+ + e^-]^{3+}$ (peak marked in green in the mobilogram in Figure 3c). The fragmentation of $[3_1^1\mathbf{F} - 2H^+ + e^-]^{3+}$ that now occurred more easily due to the presence of a radical center resulted in the cleavage of a covalent bond and a gradual unfolding of the knot. The mobilogram reveals the formation of a number of conformers with the same *m/z* as the trefoil knot, but with longer drift times (peaks marked in grey in Figure 3c). Finally, the unfolded linear fragment $[0_1^0\mathbf{F} - 2H^+ + e^-]^{3+}$ was observed (peak marked in yellow in Figure 3c). Therefore, following the energy-resolved gradual unfolding of the structure with TWIMS also allowed clear-cut assignment of the topology of a knot.

With the fragmentation patterns matching expectation, the question remains of how to distinguish a Solomon link from a Hopf link or a trefoil knot from a macrocycle. The floppiness factors *Fl* defined above should provide more information (Figure 4).

Although the *Fl* values for the Hopf links present in our libraries were close to those obtained for the Solomon links (see Table S1), they are somewhat higher, but should be treated as a guideline rather than a strict proof. More clearly, the *Fl* values obtained for all macrocycles under study were clearly higher than the *Fl* values for the trefoil knot. Consequently, consideration of CID/IMS/MS together with the floppiness factor *Fl* provides a straightforward assignment of the molecular topologies.

Furthermore, it is of interest whether the same methodology can be applied to the analysis of catenanes, which (i) do not consist of identical interlocked rings and (ii) contain a templating metal ion. The library **PyCat** contained a macrocycle ($0_1^1\mathbf{L}$, see structure in Figure S31), a Pd(II)-templated [2]catenate ($2_1^2\mathbf{PyCat}$), and a [3]catenate ($4_1^3\mathbf{PyCat}$).[25] The Pd(II)-templated [3]catenate ion $[4_1^3\mathbf{PyCat}]^{4+}$ has twice the mass and twice the charge of the Hopf link $[2_1^2\mathbf{PyCat}]^{2+}$ and, therefore, could not be separated solely based on the *m/z* value. However, in TWIMS these species were well separated (see Figure S29) and were subjected to CID separately. Here, the positive charges are carried by the palladium cation coordinated inside the catenate; hence, predicting fragmentation pathways for these structures is more difficult. For Hopf link $[2_1^2\mathbf{PyCat}]^{2+}$ we observed a selective cleavage of one of the rings together with a charge transfer reaction (Figure S29). Therefore, the formation of both the open $[0_1^0\mathbf{PyMc} - e^-]^{1+}$ and closed $[0_1^1\mathbf{L} + e^-]^{1+}$ macrocycle could be observed with TWIMS. This example demonstrates that CID/TWIMS/MS experiment is also feasible for assigning the topology of metal-templated [2]catenates and unsymmetrical catenates.

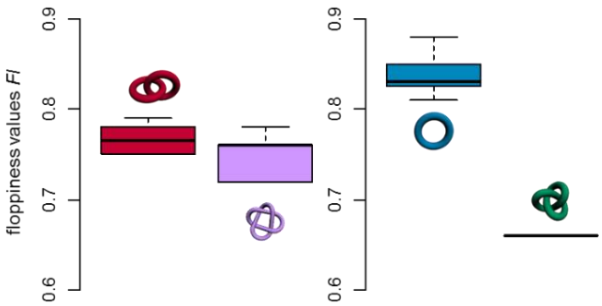

Figure 4. A boxplot showing the distribution of floppiness values *Fl* for the six Hopf links (left, red), the two Solomon links at different charge states (left, violet), the eight macrocycles (right, blue), and the trefoil knot (right, green). The "box" shows the 50% of the range of *Fl* values, while the thick line shows the median.

In case of the [3]catenate ion $[4_1^3\mathbf{PyCat}]^{4+}$, two fragmentation pathways can occur: (i) the formation of [2]catenate $2_1^2\mathbf{PyCatL}$ (see structure in Figure S31) together with an open terminal macrocycle $0_1^0\mathbf{PyMc}$ in a 1:1 ratio or (ii) the formation of closed-terminal macrocycles $0_1^1\mathbf{PyMc}$ and the open central macrocycle

$0_1^0\mathbf{L_2}$ in a 2:1 ratio (Figure 1). Here, the first fragmentation pathway occurred exclusively, together with a charge transfer (see Figure S30) and, therefore, also the topology of the [3]catenate could be assessed.

In summary, CID/IMS/MS has been demonstrated to be a versatile analytical tool for assigning the topology of molecular catenanes and knots without the need for computational modelling of the structures. We were able to assign the topology of six Hopf links, two Solomon links, a [3]catenate, and a trefoil knot. After collision-induced covalent bond cleavage, the [2]catenanes underwent dissociation into a linear and a cyclic fragment, while a knot reacted through covalent bond cleavage and gradually unfolded into a linear form. We have also developed the floppiness factor *Fl* to assign the topology of various structures. This parameter is in agreement with the assumption that Solomon links are more tightly packed than Hopf links, and that the trefoil knot is clearly more compact than any of the macrocycles. We anticipate our methods to be of use in assigning even complex topologies, in particular, when they are difficult to separate from mixtures and thus difficult to crystallize and to characterize by spectroscopic methods due to signal superpositions.

Acknowledgements

We are grateful to the Deutsche Forschungsgemeinschaft (CRC 765 “Multivalency”) for funding and the Alexander von Humboldt Foundation for a postdoctoral fellowship to A.K. The Swiss National Science Foundation (PZ00P2_161270) and the Department of Organic Chemistry at the University of Geneva are also acknowledged for their support. Financial support was also provided by the European Research Council (695009) and the UK Engineering and Physical Sciences Research Council (EPSRC, EP/P027067/1). R.L. was funded by the Fondation Wiener-Anspach postdoctoral fellowship.

Keywords: tandem mass spectrometry • ion mobility spectrometry • intertwined molecules • Solomon link • trefoil knot

[1] C. J. Bruns, J. F. Stoddart, in *Beauty Chem.* (Ed.: L. Fabbrizzi), Springer Berlin Heidelberg, Berlin, Heidelberg, **2011**, pp. 19–72.
[2] R. S. Forgan, J.-P. Sauvage, J. F. Stoddart, *Chem. Rev.* **2011**, *111*, 5434–5464.
[3] J. Arsuaga, M. Vazquez, P. McGuirk, S. Trigueros, D. W. Sumners, J. Roca, *Proc. Natl. Acad. Sci.* **2005**, *102*, 9165–9169.
[4] P. Dabrowski-Tumanski, J. I. Sulkowska, *Proc. Natl. Acad. Sci.* **2017**, *114*, 3415–3420.
[5] J.-F. Ayme, J. E. Beves, C. J. Campbell, D. A. Leigh, *Angew. Chem. Int. Ed.* **2014**, *53*, 7823–7827.
[6] N. H. Evans, *Chem. - Eur. J.* **2018**, *24*, 3101–3112.
[7] L. Zhang, A. J. Stephens, A. L. Nussbaumer, J.-F. Lemonnier, P. Jurček, I. J. Vitorica-Yrezabal, D. A. Leigh, *Nat. Chem.* **2018**, *10*, 1083–1088.
[8] J. J. Danon, D. A. Leigh, S. Pisano, A. Valero, I. J. Vitorica-Yrezabal, *Angew. Chem. Int. Ed.* **2018**, *57*, 13833–13837.
[9] F. Vögtle, A. Hünten, E. Vogel, S. Buschbeck, O. Safarowsky, J. Recker, A.-H. Parham, M. Knott, W. M. Müller, U. Müller, et al., *Angew. Chem. Int. Ed.* **2001**, *40*, 2468–2471.
[10] G. Gil-Ramírez, D. A. Leigh, A. J. Stephens, *Angew. Chem. Int. Ed.* **2015**, *54*, 6110–6150.
[11] S. D. P. Fielden, D. A. Leigh, S. L. Woltering, *Angew. Chem. Int. Ed.* **2017**, *56*, 11166–11194.
[12] J.-M. Lehn, *Chem. - Eur. J.* **1999**, *5*, 2455–2463.
[13] S. P. Black, D. M. Wood, F. B. Schwarz, T. K. Ronson, J. J. Holstein, A. R. Stefankiewicz, C. A. Schalley, J. K. M. Sanders, J. R. Nitschke, *Chem. Sci.* **2016**, *7*, 2614–2620.
[14] T. Prakasam, R. A. Bilbeisi, R. El-Khoury, L. J. Charbonnière, M. Elhabiri, G. Esposito, J.-C. Olsen, A. Trabolsi, *Dalton Trans.* **2017**, *46*, 16474–16479.
[15] C. D. Pentecost, K. S. Chichak, A. J. Peters, G. W. V. Cave, S. J. Cantrill, J. F. Stoddart, *Angew. Chem. Int. Ed.* **2007**, *46*, 218–222.
[16] C. A. Schalley, P. Ghosh, M. Engeser, *Int. J. Mass Spectrom.* **2004**, *232*, 249–258.
[17] M. Ammann, A. Rang, C. A. Schalley, P. Bäuerle, *Eur. J. Org. Chem.* **2006**, 1940–1948.
[18] P. Bäuerle, M. Ammann, M. Wilde, G. Götz, E. Mena-Osteritz, A. Rang, C. A. Schalley, *Angew. Chem. Int. Ed.* **2007**, *46*, 363–368.
[19] W. Zhang, A. Abdulkarim, F. E. Golling, H. J. Räder, K. Müllen, *Angew. Chem.* **2017**, *129*, 2689–2692.
[20] C. A. Schalley, J. Hoernschemeyer, X. Li, G. Silva, P. Weis, *Int. J. Mass Spectrom.* **2003**, *228*, 373–388.
[21] K. Caprice, M. Pupier, A. Kruve, C. A. Schalley, F. B. L. Cougnon, *Chem. Sci.* **2018**, *9*, 1317–1322.
[22] G. Wu, C.-Y. Wang, T. Jiao, H. Zhu, F. Huang, H. Li, *J. Am. Chem. Soc.* **2018**, *140*, 5955–5961.
[23] F. B. L. Cougnon, K. Caprice, M. Pupier, A. Bauzá, A. Frontera, *J. Am. Chem. Soc.* **2018**, *140*, 12442–12450.
[24] C. A. Schalley, C. Verhaelen, F.-G. Klärner, U. Hahn, F. Vögtle, *Angew. Chem. Int. Ed.* **2005**, *44*, 477–480.
[25] C. Browne, T. K. Ronson, J. R. Nitschke, *Angew. Chem. Int. Ed.* **2014**, *53*, 10701–10705.

COMMUNICATION

Cutting the Gordian knot:
Collision-induced dissociation and travelling-wave ion mobility mass spectrometry together provide a fast screening method to identify the topology of molecular Hopf and Solomon links, a [3]catenate and a trefoil knot, even when they coexist in quickly equilibrating dynamic covalent libraries.

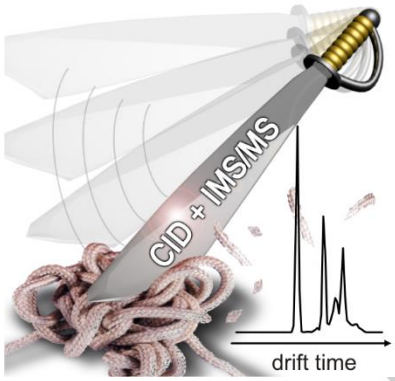

*Anneli Kruve, Kenij Caprice, Roy Lavendomme, Jan M. Wollschläger, Stefan Schoder, Hendrik V. Schröder, Jonathan R. Nitschke, Fabien B. L. Cougnon and Christoph A. Schalley**

Page No. – Page No.
Ion Mobility Mass Spectrometry for the Rapid Determination of the Topology of Interlocked and Knotted Molecules